RESEARCH ARTICLE

A splice-site variant (c.3289-1G>T) in *OTOF* underlies profound hearing loss in a Pakistani kindred

Ashfaque Ahmed[1], Meng Wang[1], Rizwan Khan[1], Abid Ali Shah[1], Hui Guo[1], Sajid Malik[2*], Kun Xia[1*] and Zhengmao Hu[1,3*]

Abstract

Background: Hearing loss/deafness is a common otological disorder found in the Pakistani population due to the high prevalence of consanguineous unions, but the full range of genetic causes is still unknown.

Methods: A large consanguineous Pakistani kindred with hearing loss was studied. Whole-exome sequencing and Sanger sequencing were performed to search for the candidate gene underlying the disease phenotype. A minigene assay and reverse transcription polymerase chain reaction was used to assess the effect of splicing variants.

Results: The splicing variants of *OTOF* (NM_194248, c.3289-1G>T) cosegregated with the disease phenotype in this Pakistani family. The substitution of a single base pair causes the deletion of 10 bp (splicing variant 1) or 13 bp (splicing variant 2) from exon 27, which results in truncated proteins of 1141 and 1140 amino acids, respectively.

Conclusion: Our findings reveal an *OTOF* splice-site variant as pathogenic for profound hearing loss in this family.

Keywords: Hearing loss, *OTOF*, Splice acceptor site, Minigene

Background

Hearing loss is characterized by any degree (mild, moderate, severe, or profound) of loss of the ability to hear that can occur at any stage of life [1, 2]. Congenital hearing loss is the fourth highest cause of disability globally with a prevalence ranging from 0.2 to 1% among newborns worldwide [3, 4]; currently, there are approximately 466 million people with hearing loss [5]. In Pakistan, hereditary deafness covers 70% of cases, and autosomal recessive hearing impairment accounts most due to the high

rate of consanguineous marriages [6]. Generally, hearing loss is classified into syndromic or non-syndromic, based on whether accompanied by other organ disorders [1]. Nonsyndromic hearing loss (NSHL) can categorized as prelingual and post lingual deafness. In the prelingual NSHL category, the proportion of inheritance pattern varies, with autosomal recessive about 75–80%, dominant 20–25% and X-linked 1–1.5% [7]. To date, at least 70 genes and 89 loci for autosomal recessive nonsyndromic hearing loss (ARNSHL) have been discovered (http://hereditaryhearingloss.org). Nongenetic factors such as congenital cytomegalovirus, toxoplasmosis, asphyxia, and exposure to noise or ototoxic drugs can also cause hearing loss. A variety of genes are implicated in hearing loss, such as the gap junction protein2 (GJB2), the potassium voltage-gated channel subfamily Q member 4 (*KCNQ4*) and OTOF [7]. The *OTOF* gene, located on chromosome 2p23.3, measures 90 kb and contains 48

*Correspondence: malik@qau.edu.pk; xiakun@sklmg.edu.cn; huzhengmao@sklmg.edu.cn
[1] Center for Medical Genetics and Hunan Key Laboratory of Medical Genetics, School of Life Sciences, Central South University, Changsha 410078, Hunan, China
[2] Human Genetics Program, Department of Zoology, Faculty of Biological Sciences, Quaid-I-Azam University, Islamabad, Pakistan
Full list of author information is available at the end of the article

Ahmed *et al. BMC Med Genomics*   (2021) 14:2

Page 2 of 8

coding exons [8]. Otoferlin (OMIM; 603,681) protein, encoded by *OTOF*, is a Ca^{2+}-binding transmembrane protein of synaptic vesicles which play a crucial part in maintaining exocytosis and vesicle priming at the ribbon synapses of cochlear inner hair cell [9, 10]. DFNB9 (OMIM; 601,071) is an ARNSHL caused by *OTOF* mutations, affecting the function of hair cell in the inner ear and the neurotransmission of auditory signal [11, 12]. A previous study indicated that *OTOF* mutations were the genetic cause in 13 (2.3%) of 557 Pakistani families with hereditary deafness [13], and a recent study showed that *OTOF* mutations was responsible for moderate to severe hearing loss in 4.4 percent of people in Pakistan [14]. The invariant GT and AG dinucleotides in the 5′ and 3′ splice sites are of importance as their mutations generally lead to human genetic diseases [15]. Here, we report an *OTOF* gene splicing acceptor site (NM_194248): c.3289-1G>T mutation that caused profound hearing loss in a large consanguineous Pakistani family.

Methods
Family and clinical examination
The consanguineous family, recruited from rural suburbs in southern Pakistan, included the two phenotypes of intellectual disability and deafness, but none of the patients showed both phenotypes. Subjects with intellectual disability showed axonal polyneuropathy and other physical features [16]. There were seven deaf patients (four males and three females) in this five-generation pedigree. The affected subjects segregated in the fourth and fifth generations in a manner that suggested an autosomal recessive inheritance pattern (Fig. 1a). The clinical evaluations included pure-tone audiometry (PTA) at 125–8 kHz in a quiet room and impedance audiometry or tympanometry of six affected individuals (IV-2, IV-4, IV-5, IV-9, V-2, V-11) and one unaffected individual (IV-16). A brain stem evoked response audiometry (BERA) test was performed for subject V-10 (Additional file 1). Written informed consent was obtained from the family elders under the regulations of the Institutional Review Board of the School of Life Sciences, Central South University, and Quaid-i-Azam University Islamabad.

Whole-exome sequencing (WES) and data analysis
Blood samples were collected from 7 affected and 28 unaffected subjects in the family in 5 ml EDTA tubes (Fig. 1a). Genomic DNA was extracted from leukocytes of all recruited family members using the Wizard Genomic DNA Purification Kit (Promega A1620). The quality of DNA was checked on a Nanospec Cube Biophotometer (Nanolytik, Dusseldorf, Germany). Whole-exome sequencing (WES) was performed on one microgram genomic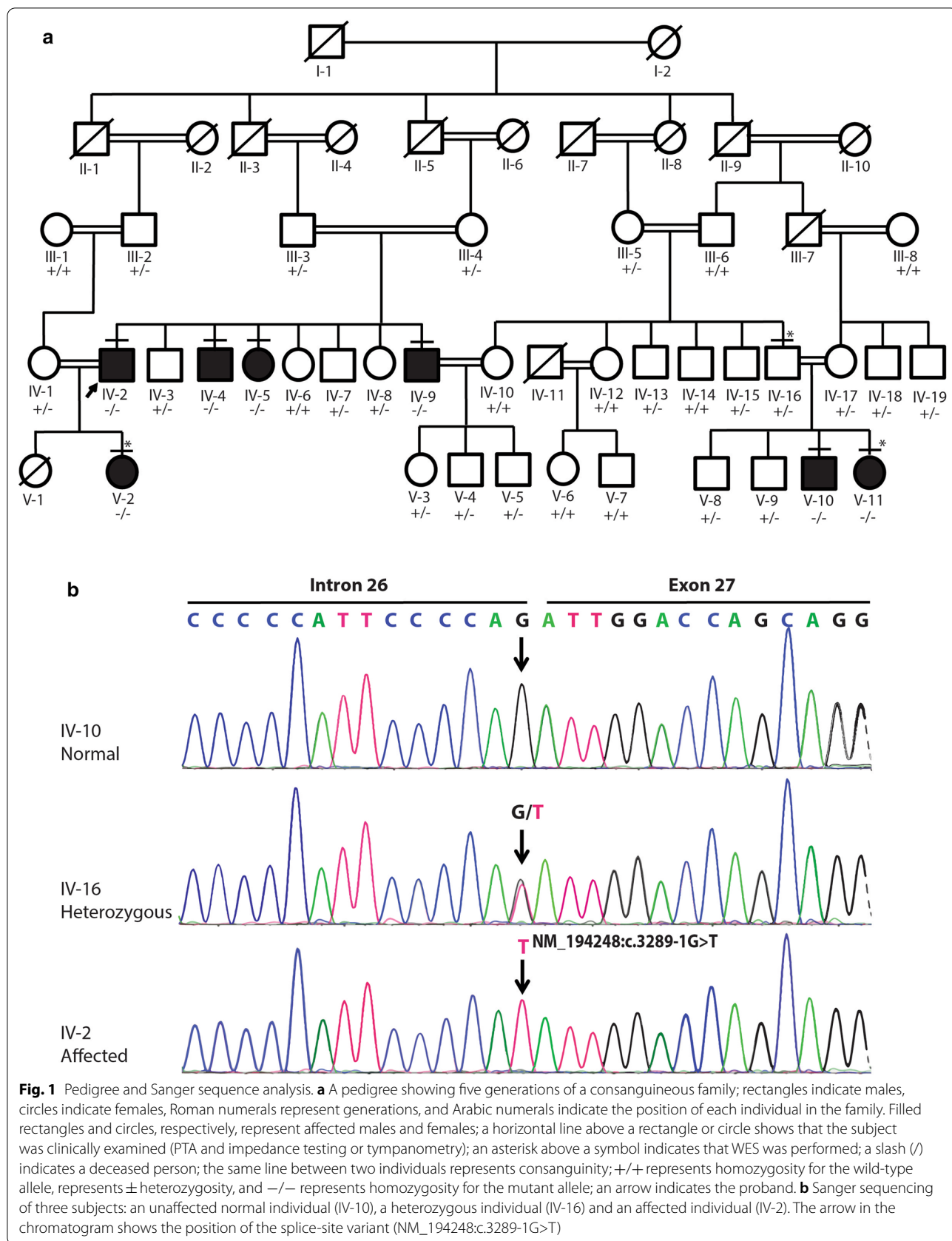 DNA samples from two affected (V-2, V-11) and one unaffected individual (IV-16) using the Agilent Sure-Select Target Enrichment System (V6) and the Illumina X Ten platform. Generated reads were aligned to human reference genome GRCH37/hg19 using Burrows-Wheeler Aligner (version 0.7.12-r1044). Variants were called by GATK (version 3.5) and annotated by ANNOVAR (version 2015-06-17). We filtered WES data variants as the strategy in Ahmed et al. [16] and excluded the variants with allele frequencies > 0.01 as reported in the GnomAD, Exome Aggregation Consortium (ExAC), 1000 Genome and ESP6500 databases. Missense mutations, nonsense mutations and splicing variants were evaluated. Sorting Intolerant from Tolerant (SIFT), Polymorphism Phenotyping V.2 (PolyPhen-2), and Mutation Taster were used to assess the overall impact of the variant selected for Sanger analysis.

Sanger sequence analysis of the selected gene variant
Primers were designed with Primer3 to validate the selected variant (NM_194248: c.3289-1G>T) from WES data through Sanger sequencing. The primer sequences were as follows: forward, 5′-cgtggtccttagggggttt-3′; reverse, 5′-gagtgcgacttggtgcagat-3′. PCR amplification was performed with these primers for all available individuals by using the GeneAmp PCR system 2720 (Applied Biosystems, Foster City, CA, USA). The PCR mix consisted of 5 µl of premix ExTaq Polymerase (Takara Bio, Dalian, China), 30 ng of DNA, 50 ng of primers, and ddH_2O for a total volume of 10 µl. The PCR conditions were as follows: an initial denaturing step at 95 °C; 35 cycles of denaturing at 95 °C for 1 min, annealing at 58 °C for 1 min, and extension at 72 °C for 1 min; and a final extension step at 72 °C for 10 min. The PCR products were verified by 1% polyacrylamide gel electrophoresis and ethidium bromide (EB) staining, after which Sanger sequencing was performed. Sequence traces were visualized with CodonCode Aligner (Version 7.1.2) and SeqMan (Lasergene).

Minigene design and plasmid construction
A minigene splicing assay was performed as previously described [17]. In order to assess the impact of the detected sequence variant on splicing, a minigene assay was performed for exons 25–29 of *OTOF* (Fig. 3a). The primers were designed with Primer-Blast (https://www.ncbi.nlm.nih.gov/tools/primer-blast), and the sequences were as follows: forward, 5′-TTG GCGCGCCCTCTGGCTTTGAGAGCACCAG-3′; reverse, 5′-ATAAGAATGCGGCCGCAGCCTGAC TGGACAGATGGAT-3′. The genomic DNA (gDNA) of the unaffected heterozygous individual IV-16 was amplified using Phanta Max Super-Fidelity DNA polymerase (p505-d1/d2/d3, Vazyme, Nanjing, Jiangsu,

Ahmed *et al. BMC Med Genomics*   (2021) 14:2

Page 3 of 8

Fig. 1 Pedigree and Sanger sequence analysis. **a** A pedigree showing five generations of a consanguineous family; rectangles indicate males, circles indicate females, Roman numerals represent generations, and Arabic numerals indicate the position of each individual in the family. Filled rectangles and circles, respectively, represent affected males and females; a horizontal line above a rectangle or circle shows that the subject was clinically examined (PTA and impedance testing or tympanometry); an asterisk above a symbol indicates that WES was performed; a slash (/) indicates a deceased person; the same line between two individuals represents consanguinity; +/+ represents homozygosity for the wild-type allele, represents ± heterozygosity, and −/− represents homozygosity for the mutant allele; an arrow indicates the proband. **b** Sanger sequencing of three subjects: an unaffected normal individual (IV-10), a heterozygous individual (IV-16) and an affected individual (IV-2). The arrow in the chromatogram shows the position of the splice-site variant (NM_194248:c.3289-1G>T)

Ahmed *et al. BMC Med Genomics*   (2021) 14:2

Page 4 of 8

China) with the appropriate primers and then introduced into the pCAGGS-IRES-green fluorescent protein (GFP) vector by Sgsl and NOT1 (ER1892 and FD0596, Thermo Fisher Scientific, Waltham, MA, USA). The plasmid was used to transform *E. coli* DH5α (CB101-2, Tiangen, Beijing, China). Ten positive clones were selected on Luria–Bertani (LB) plates, and the genotypes of the clones were confirmed by Sanger sequencing. After sequence alignment, wild-type and mutant plasmids were selected to transfect cell lines.

Cell culture and transfection
Human embryonic kidney (HEK) 293 cells and HeLa cells were maintained in DMEM (Gibco-BRL Life Technologies, Grand Island, NY) containing 10% fetal bovine serum (FBS) (Gibco-BRL Life Technologies). Cells were grown in 24-well plates at 37 °C in a 5% CO_2 atmosphere. Wild-type and mutant plasmids in an otherwise similar construct were transfected into HEK 293 cells and HeLa cell using Lipofectamine 3000 reagent (L3000008, Invitrogen, Carlsbad, CA, USA).

Reverse transcription PCR
After 24 h, RNA was extracted from the cells using the FastPure Cell/Tissue Total RNA Isolation Kit (RC101-01, Vazyme, Nanjing, Jiangsu, China). cDNA was generated from 500 ng of total RNA using a RevertAid First Strand cDNA Synthesis Kit (K1621, Thermo Fisher Scientific, Waltham, MA, USA). The primer sequences were as follows: forward, 5′-GTGCTGAATGAGACCCTGTG-3′; reverse, 5′-CCGTGGTGTTCCAGCTGGGG-3′. PCRs were generated using Phanta Max Super-Fidelity DNA polymerase (p505-d1/d2/d3, Vazyme). The amplification was performed for 35 cycles of 72 °C for 1 min, 62 °C for 30 s, and 72 °C for 1 min.

Construction of the pMD-19T plasmid
The final product was introduced into the plasmid vector pMD19-T using a DNA ligation kit (D102A, Thermo Fisher Scientific, Waltham, MA, USA). Then, the plasmid was used to transform DH5α cells (CB101-2, Tiangen, Beijing, China). The positive clones were selected by blue/white screening on Luria–Bertani (LB) plates; ten successful clones from HEK 293 cells and ten from HeLa cells were confirmed by Sanger sequencing.

Results
Clinical findings
The ages of the seven affected subjects ranged from 1 to 28 years, and these subjects presented congenital, symmetrical bilateral hearing impairment. No malformation of any other organ system was evident in the fourth or fifth generation of the pedigree (Fig. 1a). PTA of six affected individuals (IV-2, IV-4, IV-5, IV-9, V-2, and V-11) and one unaffected individual (IV-16) showed readings of ≥ 90 dB, while the BERA test of V-10 revealed bilateral sensorineural hearing loss (Table 1, Fig. 2a, Additional file 1A); the tympanograms were of the normal type, 'A', in all tested ears except the right ears of two subjects (IV-5, IV-9), which had type 'As' tympanograms (Table 1, Fig. 2b, and Additional file 1B). Pedigree and clinical results suggested that it is a profound type of ARNSHL, as per the criteria of the American Speech-Language-Hearing Association (ASHA 2015).
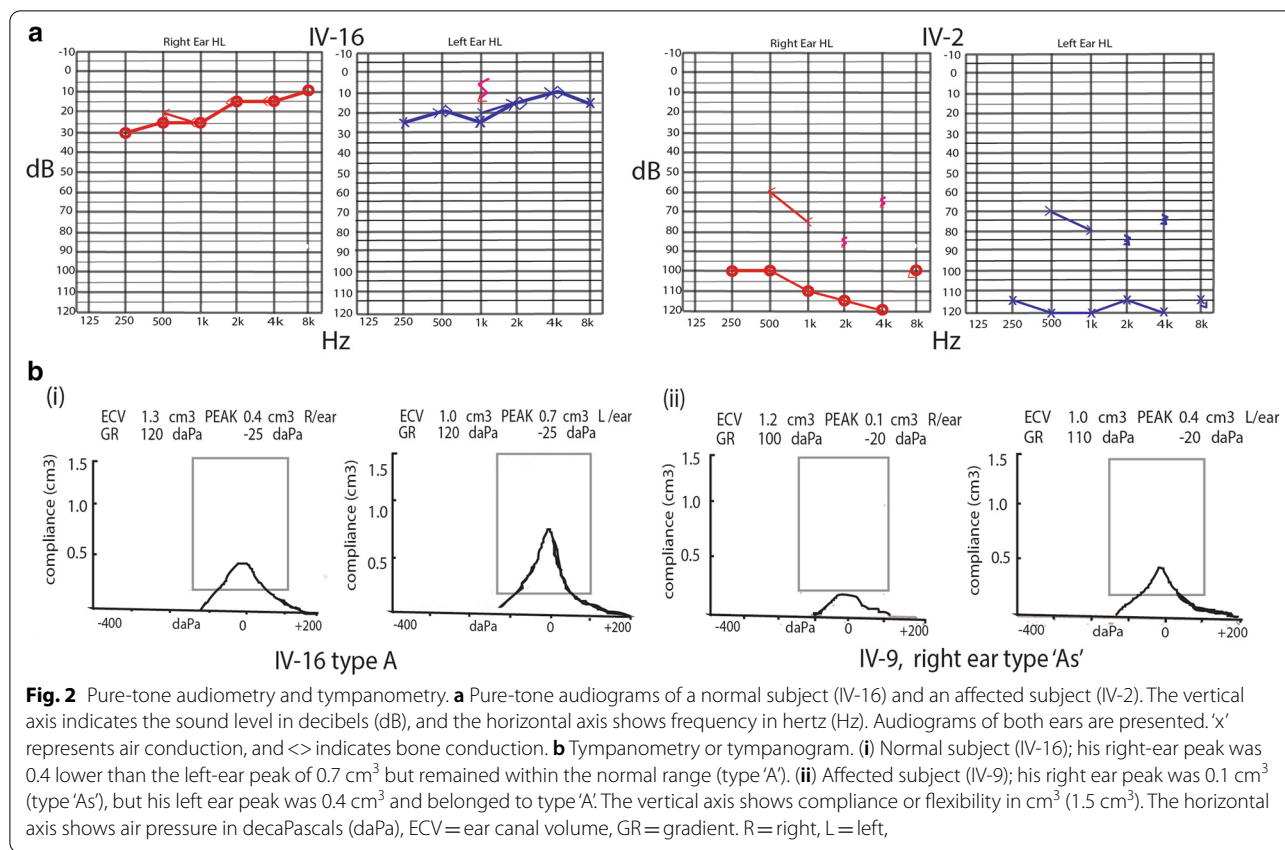
Whole-exome sequencing and Sanger analysis
After the filtering strategy was applied to the WES data (see Methods), 209 variants were found in the affected subject V-2, 210 in the affected subject V-11, and 193 in the unaffected subject IV-16. Six possible candidate variants (CRISPLD2:NM_031476:c.1292A>G:p. N431S, ADCY3:NM_004036: c. 557 G>A: p.S186N, OTOF:NM_194248:c.3289-1G>T,

Table 1 Clinical evaluations of assessed subjects/patients

Ped. ID	Sex	Age (years)	Status	Clinical test	PTA (dB)	Imp: type		Severity	Diagnosis
						R. ear	L. ear		
IV-16	M	29	N	PTA and Imp	≤ 30	A	A	Normal	Normal
IV-2	M	28	A	PTA and Imp	≥ 100	A	A	Profound	ARNSHL
IV-4	M	27	A	PTA and Imp	≥ 90	A	A	Profound	ARNSHL
IV-5	F	12	A	PTA and Imp	≥ 100	As	A	Profound	ARNSHL
IV-9	M	26	A	PTA and Imp	≥ 100	As	A	Profound	ARNSHL
V-2	F	5	A	PTA and Imp	≥ 105	A	A	Profound	ARNSHL
V-10	M	1	A	BERA	Nil	Nil	Nil	Profound	ARNSHL
V-11	F	9	A	PTA and Imp	≥ 100	A	A	Profound	ARNSHL

M: male; F: female; N: normal; A: affected; PTA: pure-tone audiometry; Imp: impedance (tympanometry); type 'A' or type 'As'; BERA: brain stem emission response audiogram

Fig. 2 Pure-tone audiometry and tympanometry. **a** Pure-tone audiograms of a normal subject (IV-16) and an affected subject (IV-2). The vertical axis indicates the sound level in decibels (dB), and the horizontal axis shows frequency in hertz (Hz). Audiograms of both ears are presented. 'x' represents air conduction, and <> indicates bone conduction. **b** Tympanometry or tympanogram. (**i**) Normal subject (IV-16); his right-ear peak was 0.4 lower than the left-ear peak of 0.7 cm³ but remained within the normal range (type 'A'). (**ii**) Affected subject (IV-9); his right ear peak was 0.1 cm³ (type 'As'), but his left ear peak was 0.4 cm³ and belonged to type 'A'. The vertical axis shows compliance or flexibility in cm³ (1.5 cm³). The horizontal axis shows air pressure in decaPascals (daPa), ECV = ear canal volume, GR = gradient. R = right, L = left,

CIB4:NM_001029881:c.364C>G: p.L122V, RGPD4:NM_182588:c.2468A>T:p.K823M, PPP2R2B:NM_181675:c.57_58insAG CAGCAGCAG CAGCAGCAGC:p.C20delinsSSSSSSSC) were present in both affected subjects but not in the unaffected individual. The candidate gene *OTOF* has already been reported to be associated with a hearing loss phenotype matching this family's phenotype, and the allele frequency (NM_194248: c.3289-1G>T) is 0.000004 (allele count: 1 out of 249,936) according to the GnomAD databases. Sanger sequencing was implemented to validate the variant in all family members; the variant was found to cosegregate with the phenotype of hearing loss in the pedigree (Fig. 1).
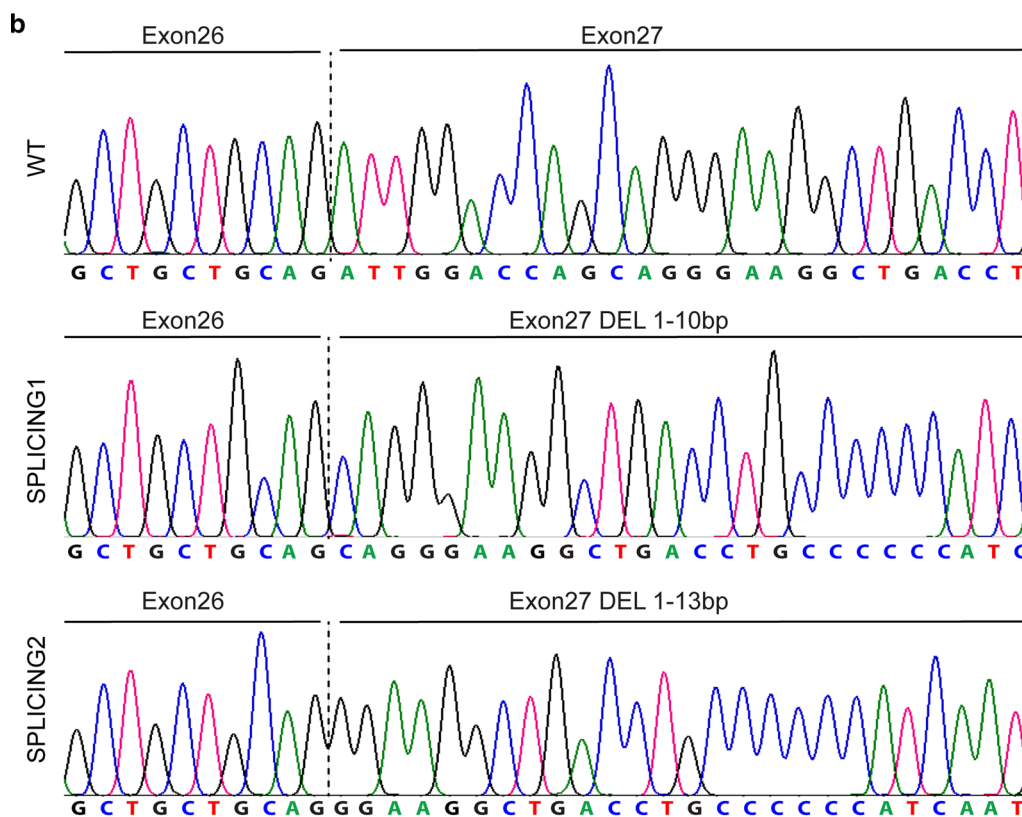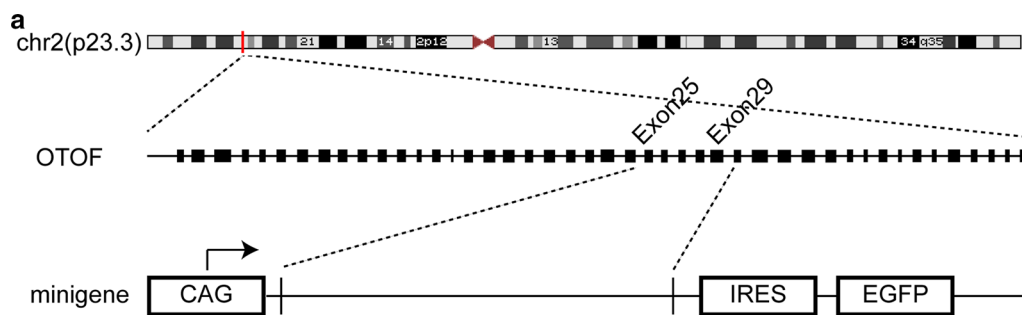
Minigene assay for splicing mutation

A minigene assay and reverse transcription PCR analysis confirmed the normal splicing of messenger RNA in exon 27 with the wild-type allele. Two predominant splicing variants of *OTOF* are produced through the c.3289-1G>T variation in the intron 26 splice acceptor site: splicing variant 1, p.Ile1097Glnfs45, is a 10 bp deletion with the sequence ATTGGACCAG; splicing variant 2, p.Ile1097Glyfs44, is a 13 bp deletion with the sequence ATTGGACCAAGCAG (Fig. 3b). The splicing assay indicated that the c.3289-1G>T mutated minigene produces these two spliced transcripts, which cause a frameshift that result in an early termination of protein expression in both HEK 293 and HeLa cell lines, and splicing variant

(See figure on next page.)
Fig. 3 Minigene assay for the targeted variant. **a** Minigene construction; the vertical dashed red line shows the position of *OTOF* on chromosome 2p23.3. The next dashed underline represents *OTOF*, including its introns and exons. The minigene target sequence is from exon 25 to exon 29; this sequence was cloned in a CAGGS plasmid with internal ribosome entry sites (IRES), and enhanced green fluorescent protein (EGFP). **b** Sanger sequencing of the wild type (WT) and the mutant for splicing variants 1 and 2; the dashed line indicates the exon junction between exons 26 and 27. Splicing variant 1 deleted 1–10 bp from exon 27, and splicing variant 2 deleted 1–13 bp from the same exon. **c** The protein translation of the WT sequence and splicing variants 1 and 2. The splicing acceptor site mutation produced truncated proteins of 1141 amino acids (p.Ile1097Glnfs45) in splicing variant 1 and 1140 amino acids (p.Ile1097Glyfs44) in splicing variant 2, instead of the normal mature protein of 1998 amino acids. Ile = isoleucine, Gln = glutamine, Gly = glycine

Ahmed *et al. BMC Med Genomics*   (2021) 14:2

Page 6 of 8

a
chr2(p23.3)

OTOF

minigene | CAG | ... | IRES | EGFP

Exon25 Exon29

b

	Exon26	Exon27
WT		

G C T G C T G C A G A T T G G A C C A G C A G G G A A G G C T G A C C T

	Exon26	Exon27 DEL 1-10bp
SPLICING1		

G C T G C T G C A G C A G G G A A G G C T G A C C T G C C C C C C A T C

	Exon26	Exon27 DEL 1-13bp
SPLICING2		

G C T G C T G C A G G G A A G G C T G A C C T G C C C C C C A T C A A T

c

	Leu	Leu	Gln	IIE	Gly	Pro	Ala	Gly	Lys	Ala	⋯⋯	Ala	Stop
	1094	1095	1096	1097	1098	1099	1100	1101	1102	1103	⋯⋯	1997	1998
WT	CTG	CTG	CAG	ATT	GGA	CCA	GCA	GGG	AAG	GCT	⋯⋯	GCC	TGA

	Leu	Leu	Gln	Gln	Gly	Arg	Leu	Thr	Cys	Pro	⋯⋯	Thr	Stop
	1094	1095	1096	1097	1098	1099	1100	1101	1102	1103	⋯⋯	1141	1142
SPLICING1	CTG	CTG	CAG	CAG	GGA	AGG	CTG	ACC	TGC	CCC	⋯⋯	ACC	TAA

	Leu	Leu	Gln	Gly	Arg	Leu	Thr	Cys	Pro	Pro	⋯⋯	Thr	Stop
	1094	1095	1096	1097	1098	1099	1100	1101	1102	1103	⋯⋯	1140	1141
SPLICING2	CTG	CTG	CAG	GGA	AAG	CTG	ACC	TGC	CCC	CCA	⋯⋯	ACC	TAA

2 was 3- to 4-fold more common than splicing variant 1. The expression of splicing variant 1 and splicing variant 2 was predicted with Snap gene (http://www.snapgene.com/) (Fig. 3c).

Discussion

According to the guidelines in the ACMG [1], all patients with hearing loss in this large consanguineous family were found to have pre-lingual profound deafness by a clinical examination including PTA and tympanometry. The WES results of three subjects (IV-16, V-2, and V-11) identified a splicing mutation (NM_194248: c.3289-1G>T; exon 27) in the *OTOF* gene that caused profound deafness/hearing loss. Previous studies have also shown that *OTOF* mutation causes profound hearing loss. In a recent cohort study, *OTOF* was found to contribute most to AR hearing loss in the Saudi Arabian population, responsible for 21.1% (7/11) of cases in the study population [4]. Wang et al. also reported that *OTOF* mutations cause mild, moderate, or profound hearing loss [2]. In our study, all patients suffer from bilateral profound hearing loss with PTA $\geq$ 90 dB at a frequency of 125–8 kHz (Fig. 2a, Additional file 1A). In this family, we also performed impedance testing or tympanometry to define the status of the tympanic membrane. The middle ear and impedance test results universally showed normal type 'A' tympanic membranes except in two subjects (IV-5 and IV-9), who had the 'As' type in the right ear, potentially marking progression to the abnormal state of 'otosclerosis'; none of the participants had other physical abnormalities or syndromic features (Fig. 2b, Additional file 1B).

Aberrant transcript splicing represents a common class of mutations in hearing loss. The splicing mutation NM_194248:c.3289-1G>T has been reported in *OTOF* by Naz et al. 2017 and was predicted to cause skipping of exon 27 [14]. This mutation, affecting the canonical GU-AG dinucleotides at the splice acceptor site, is highly predictive of splicing defects. This splice-site mutation may erase regular splice sites and thereby alter exon recognition. We used a minigene assay to determine how the mutation alters exon recognition. The results demonstrated that the mutation destroys the canonical acceptor site and leads to the use of alternative sites.

Otoferlin plays a major role in sustaining exocytosis and vesicle priming at the synapses of cochlear inner hair cells (IHC) [9, 10]. Otoferlin acts as a Ca^{2+} sensor to set the rates of primed vesicle fusion to replenish the presynaptic plasma membrane and synaptic vesicle pool in the active zone of IHCs [10]. Otoferlin has six C2 domains expressed in humans; from C to N terminus, these domains are as follows: C2A = 1–97 aa, C2B = 254–352 aa, C2C = 417–528 aa, C2D = 960–1067

aa, C2E = 1493–1592 aa, and C2F = 1733–1863 aa [18]. C2E and C2F interact with the syntaxin-1 t-SNARE motif, and the maximum binding occurs in the calcium range of 20–50 μM, with C2F binding to calcium directly. Calcium acts as a molecular switch regulating the opening and closing of otoferlin which is part of the mechanism of exocytosis [19]. This suggests that the C2F domain is important in the normal physiology of hearing; indeed, according to the ClinVar database (https://www.ncbi.nlm.nih.gov/clinvar/), there are 18 known C2F mutations that cause hearing loss. Our study demonstrates that the splice-site mutation produced a truncated mature otoferlin protein lacking the C2E and C2F domains, which suggests that the truncated protein could not coordinate between vesicle fusion and synaptic vesicle pool replenishment and could not function as a Ca^{2+} sensor in IHCs, which eventually disrupted the temporal precision of IHC activity and thus produced the phenotype in this pedigree.

According to ACMG standards and guidelines for the interpretation of sequence variants, this variant met the PVS1 (null variant splice site), PS3 (established by in vitro studies to have a damaging effect on the gene), PM2 (extremely low frequency if recessive), and PP1 (cosegregation with a disease in all affected subjects) criteria for pathogenicity [20], thus qualifying as a pathogenic variant.

Conclusion

The present study, through WES, Sanger sequencing, and minigene approaches, describes a splice acceptor site mutation (NM_194248: c.3289-1G>T) in *OTOF* that causes profound hearing loss; now that this splice-site variant has been implicated as pathogenic for hearing loss, the results provide evidence that that these findings will facilitate the diagnosis of deafness/hearing loss in future studies.

Supplementary Information

The online version contains supplementary material available at https://doi.org/10.1186/s12920-020-00859-x.

Additional file 1. Clinical tests performed for patients. (A). Pure-tone audiometry for IV-4, IV-5, IV-9, V-2, and V-11; BERA test for V-10. (B). Tympanometry for IV-2, IV-4, IV-5, V-2, and V-11.

Abbreviations

ACMG: American College of Medical Genetics and Genomics; PTA: Pure-tone audiometry; BERA: Stem evoked response audiometry; HEK: Human embryonic kidney; IHC: Inner hair cells.

Ahmed *et al. BMC Med Genomics*   (2021) 14:2

Page 8 of 8

Authors' contributions

Funding

Availability of data and materials

The datasets analyzed during the current study have uploaded the associated datasets of this study to the SRA—NCBI repository, the Sequence Read Archive (SRA) accession number is: PRJNA675842.

Ethics approval and consent to participate

The current study project, "The Study of Human Genetic Disorders in Pakistani Families" was conducted according to the regulations of the Institutional Review Board of the School of Life Sciences, Central South University, and the Ethical Review Board of Quaid-i-Azam University Islamabad. This study was submitted to and approved by the Ethical Review Board of Quaid-i-Azam University Islamabad. Written informed consent was obtained from the family elders/guardians with the approval of the Ethical Review Board of Quaid-i-Azam University Islamabad.

Consent for publication

Written informed consent was collected on behalf of all participants in the study (because of local customs, there was no need to obtain consent from each participant) from the elders/guardians to publish the clinical details, images, photographs, and pedigree.

Competing interests

The authors declare that they have no competing interests.

Author details

[1] Center for Medical Genetics and Hunan Key Laboratory of Medical Genetics, School of Life Sciences, Central South University, Changsha 410078, Hunan, China. [2] Human Genetics Program, Department of Zoology, Faculty of Biological Sciences, Quaid-I-Azam University, Islamabad, Pakistan. [3] Hunan Key Laboratory of Animal Models for Human Diseases, School of Life Sciences, Central South University, Changsha 410078, Hunan, China.

References

1. Alford RL, et al. American College of Medical Genetics and Genomics guideline for the clinical evaluation and etiologic diagnosis of hearing loss. Genet Med. 2014;16(4):347–55.
2. Wang Y, et al. Novel OTOF gene mutations identified using a massively parallel DNA sequencing technique in DFNB9 deafness. Acta Otolaryngol. 2018;138(10):865–70.
3. Hilgert N, Smith RJ, Van Camp G. Forty-six genes causing nonsyndromic hearing impairment: which ones should be analyzed in DNA diagnostics? Mutat Res. 2009;681(2–3):189–96.
4. Almontashiri NAM, et al. Recurrent variants in OTOF are significant contributors to prelingual nonsydromic hearing loss in Saudi patients. Genet Med. 2018;20(5):536–44.
5. Olusanya BO, Davis AC, Hoffman HJ. Hearing loss grades and the International classification of functioning, disability and health. Bull World Health Organ. 2019;97(10):725–8.
6. Meena R, Ayub M. Genetics of human hereditary hearing impairment. J Ayub Med Coll Abbottabad. 2017;29(4):671–6.
7. Vos B, et al. Newborn hearing screening programme in Belgium: a consensus recommendation on risk factors. BMC Pediatr. 2015;15:160.
8. Yasunaga S, et al. A mutation in OTOF, encoding otoferlin, a FER-1-like protein, causes DFNB9, a nonsyndromic form of deafness. Nat Genet. 1999;21(4):363–9.
9. Roux I, et al. Otoferlin, defective in a human deafness form, is essential for exocytosis at the auditory ribbon synapse. Cell. 2006;127(2):277–89.
10. Michalski N, et al. Otoferlin acts as a Ca(2+) sensor for vesicle fusion and vesicle pool replenishment at auditory hair cell ribbon synapses. Elife. 2017;6:e31013.
11. Rance G, Starr A. Pathophysiological mechanisms and functional hearing consequences of auditory neuropathy. Brain. 2015;138(Pt 11):3141–58.
12. Nishio SY, Usami SI. Outcomes of cochlear implantation for the patients with specific genetic etiologies: a systematic literature review. Acta Otolaryngol. 2017;137(7):730–42.
13. Choi BY, et al. Identities and frequencies of mutations of the otoferlin gene (OTOF) causing DFNB9 deafness in Pakistan. Clin Genet. 2009;75(3):237–43.
14. Naz S, et al. Genetic causes of moderate to severe hearing loss point to modifiers. Clin Genet. 2017;91(4):589–98.
15. Krawczak M, et al. Single base-pair substitutions in exon-intron junctions of human genes: nature, distribution, and consequences for mRNA splicing. Hum Mutat. 2007;28(2):150–8.
16. Ahmed A, et al. Biallelic loss-of-function variants in NEMF cause central nervous system impairment and axonal polyneuropathy. Hum Genet. 2020.
17. Cooper TA. Use of minigene systems to dissect alternative splicing elements. Methods. 2005;37(4):331–40.
18. Yasunaga S, et al. OTOF encodes multiple long and short isoforms: genetic evidence that the long ones underlie recessive deafness DFNB9. Am J Hum Genet. 2000;67(3):591–600.
19. Ramakrishnan NA, et al. Calcium regulates molecular interactions of otoferlin with soluble NSF attachment protein receptor (SNARE) proteins required for hair cell exocytosis. J Biol Chem. 2014;289(13):8750–66.
20. Richards S, et al. Standards and guidelines for the interpretation of sequence variants: a joint consensus recommendation of the American College of Medical Genetics and Genomics and the Association for Molecular Pathology. Genet Med. 2015;17(5):405–24.

Publisher's Note

Springer Nature remains neutral with regard to jurisdictional claims in published maps and institutional affiliations.